






Synthetic zwitterions as efficient non-permeable cryoprotectants

Yui Kato¹, Takuya Uto ², Daisuke Tanaka ³, Kojiro Ishibashi⁴, Akiko Kobayashi^{5,6}, Masaharu Hazawa^{5,6}, Richard W. Wong ^{5,6}, Kazuaki Ninomiya⁷, Kenji Takahashi¹, Eishu Hirata ^{4,6}✉ & Kosuke Kuroda ^{1,8}✉

Cryopreservation of cells is necessary for long periods of storage. However, some cell lines cannot be efficiently cryopreserved, even when optimized commercial cryoprotectants are employed. Previously, we found that a low-toxic synthetic zwitterion aqueous solution enabled good cryopreservation. However, this zwitterion solution could not cryopreserve some cells, such as human kidney BOSC cells, with good efficiency. Therefore, details of the cryoprotective effect of the zwitterions and optimization based on its mechanisms are required. Herein, we synthesized 18 zwitterion species and assessed the effects of the physical properties of water/zwitterion mixtures. Non-cell-permeable zwitterions can inhibit ice crystal formation extracellularly via direct interaction with water and intracellularly via dehydration of cells. However, cells that could not be cryopreserved by zwitterions were insufficiently dehydrated in the zwitterion solution. Dimethyl sulfoxide (DMSO) was combined as a cell-permeable cryoprotectant to compensate for the shortcomings of non-cell-permeable zwitterions. The water/zwitterion/DMSO (90/10/15, v/w/w) could cryopreserve different cells, for example freezing-vulnerable K562 and OVMANA cells; yielding ~1.8-fold cell viability compared to the case using a commercial cryoprotectant. Furthermore, molecular dynamics simulation indicated that the zwitterions protected the cell membrane from the collapse induced by DMSO.

¹Faculty of Biological Science and Technology, Institute of Science and Engineering, Kanazawa University, Kakuma-machi, Kanazawa 920-1192, Japan.

²Organization for Promotion of Tenure Track, University of Miyazaki, Nishi 1-1 Gakuen-Kibanadai, Miyazaki 889-2192, Japan. ³Genetic Resources Center, National Agriculture and Food Research Organization, Kannondai, Tsukuba 305-8602, Japan. ⁴Cancer Research Institute, Kanazawa University, Kakuma-machi, Kanazawa 920-1192, Japan. ⁵Cell-Bionomics Research Unit, Institute for Frontier Science Initiative, Kanazawa, Ishikawa 920-1192, Japan. ⁶WPI-Nano Life Science Institute, Kanazawa University, Kanazawa, Kanazawa, Ishikawa 920-1192, Japan. ⁷Institute for Frontier Science Initiative, Kanazawa University, Kakuma-machi, Kanazawa 920-1192, Japan. ⁸NanoMaterials Research Institute, Kanazawa University, Kakuma-machi, Kanazawa 920-1192, Japan.

✉email: ehirata@staff.kanazawa-u.ac.jp; kkuroda@staff.kanazawa-u.ac.jp

Cryopreservation of cells is necessary for long storage periods to avoid mutations that might ensue during cultivation. It has enabled cell banking¹. For example, >3600 cells are currently cryopreserved in the American Type Culture Collection². When cells are cryopreserved in culture media, cryoprotectants are necessary because ice crystals form intra- and intercellularly and damage cells under extremely low temperatures^{1,3–8}. A typical freezing medium is composed of medium/fetal bovine serum (FBS)/dimethyl sulfoxide (DMSO) (70/20/10, v/v/v). DMSO is cell-permeable⁹ and inhibits the formation of ice crystals intra- and extracellularly by interacting with water molecules¹⁰. However, some cell lines cannot be efficiently cryopreserved even when optimized commercial cryoprotectants are employed. Therefore, novel, efficient cryoprotectants are in high demand. However, cryoprotectants have a long research history, and their optimization has been attempted for decades without success for freezing-vulnerable cells. To break this unsuccessful cycle, the discovery of compounds that have not been applied to cryopreservation is needed.

Recently, we have developed a novel polar solvent, liquid zwitterion called OE₂imC₃C (Fig. 1), which exerts low toxicity to cells^{11–13}. Unlike amino acids, OE₂imC₃C has electric charges, as it is aprotic. This charged molecule strongly interacts with water molecules and is expected to more strongly inhibit ice crystal formation than DMSO, possessing partial charges. One of the indicators of the strength of interaction with water is hydrogen bond basicity, which is represented by the β value of the Kamlet-Taft parameters. The β values of OE₂imC₃C and DMSO are 1.12 and 0.76, respectively^{11,12}. As a result, we recently demonstrated the potential of OE₂imC₃C as a new type of cryoprotectant¹³. Water/OE₂imC₃C (95/5, v/w) cryopreserved human normal fibroblasts (hNF) and five other cell lines, as well as a DMSO-containing commercial cryoprotectant. The cryoprotective effect of OE₂imC₃C remains unclear, as it is a newly developed compound. In the present study, we carried out a detailed assessment of the limitations and potential of zwitterionic cryoprotectants, including OE₂imC₃C, and performed optimizations by analyzing the cryoprotective mechanisms employed. We revealed that cell dehydration was found to be a key factor for efficient cryopreservation. The mixtures of non-cell-permeable zwitterions and cell-permeable DMSO was found to cryopreserve freezing-vulnerable cells.

Results and discussion

Cryopreservation of cell lines with water/OE₂imC₃C (95/5, v/w). Freezing media are typically prepared with concentrations based on volume/volume using pipettes; however, OE₂imC₃C aqueous solutions (OE₂imC₃C aqs.) are difficult to prepare at volume/volume due to their high viscosity. As a result, they were prepared at volume/weight in the present study. To investigate whether water/OE₂imC₃C (95/5, v/w) can be used as a universal cryoprotectant, nine cell lines including the cells cryopreserved in the previous study, were also cryopreserved, and the relative number of living cells after thawing was counted (Fig. S1). The cryoprotective effect was found to be significantly different depending on the cell line. For example, hNFs had the highest relative number of living cells of 1.10 while the number of living cells after cryopreservation with the commercial cryoprotectant was 1.00. In contrast, the human kidney cell line (BOSC) had the lowest number (0.20). These results indicate that the differences may not be based on the parental mammal species. Here, hNF, mNF, and BOSC were subjected to further studies as good, intermediate, and poor representatives, respectively.

Optimization of the OE₂imC₃C-based freezing media. As shown above, we used a simple mixture containing OE₂imC₃C

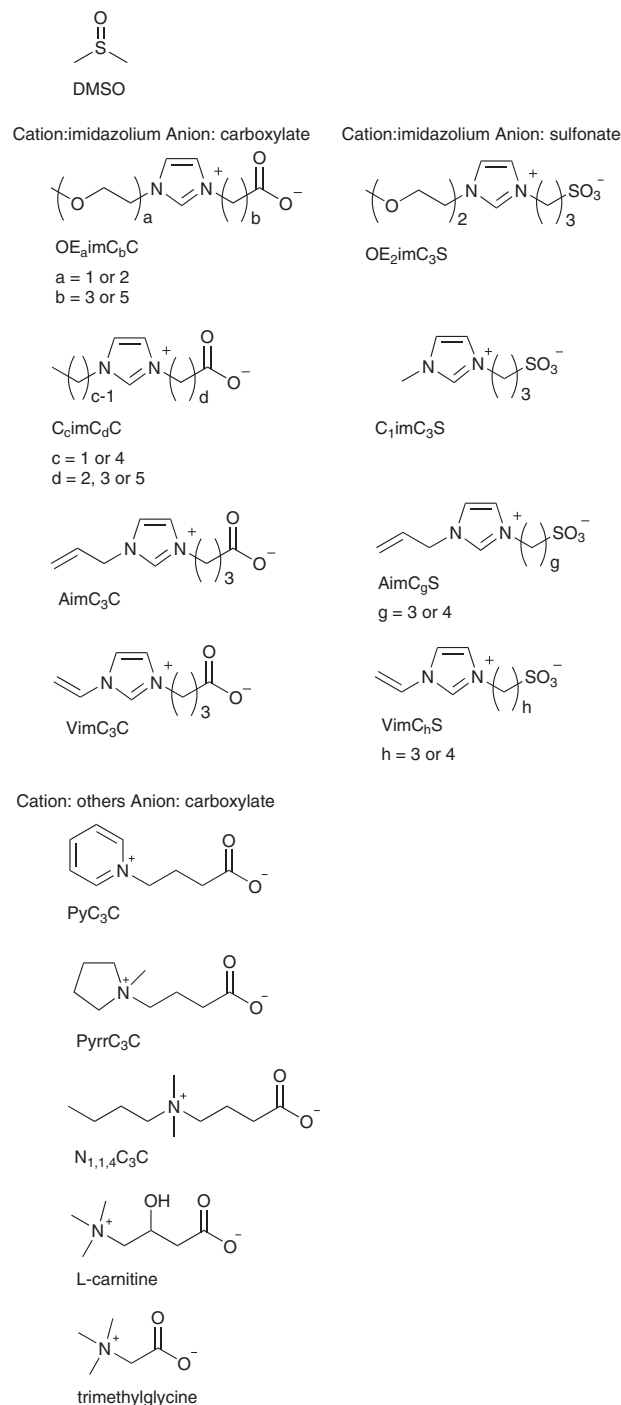


Fig. 1 Structures of DMSO and the zwitterions used in this study. They are categorized by the cation and anion species.

and water. However, based on the composition of the typical freezing medium (medium/FBS/DMSO; 70/20/10, v/v/v), we may have oversimplified this composition. Here, we carefully evaluated the components that are critical to achieve high cryopreserving efficiency relative to medium/FBS/DMSO. The relative numbers of living hNF cells after cryopreservation using medium/FBS/DMSO (70/20/10, v/v/v) and medium/FBS/OE₂imC₃C (70/20/10, v/v/w) were similar (0.99 and 0.97, respectively) (Fig. 2a). Such finding implies that OE₂imC₃C can act as an alternative to DMSO. However, the medium components critically affected the DMSO-based freezing media but not the OE₂imC₃C-based freezing media. This finding indicates that the cryopreservation

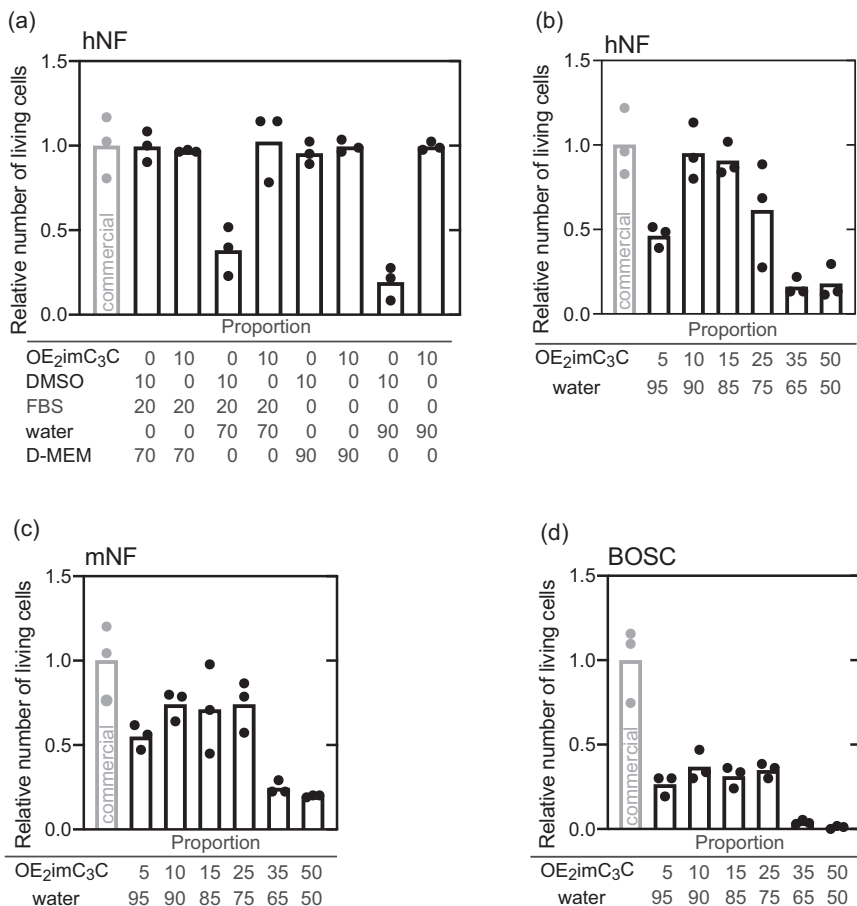


Fig. 2 Cryopreservation using OE₂imC₃C-based freezing media. Relative number of living **a**, **b** hNF, **c** mNF, and **d** BOSC cells after cryopreservation with the indicated freezing media ($n = 3$, experimentally triplicate). In this experiment, DMSO was measured in volume. The commercial cryoprotectant employed was Culture Sure freezing medium (Fujifilm Wako Pure Chemical Corporation).

mechanisms differ between DMSO- and OE₂imC₃C-based freezing media. DMSO is known as a cell-permeable cryoprotectant; however, non-cell-permeable components in media, such as NaCl, are required because the cell-permeable DMSO cannot regulate osmotic pressure, resulting in significant cell expansion (Fig. S2a). On the other hand, we reported that OE₂imC₃C hardly penetrates cells¹³. Water/OE₂imC₃C (90/10, v/w) has sufficient osmotic pressure (626 mOsm/kg) relative to the medium (Dulbecco's modified Eagle's medium with high glucose, 328 mOsm/kg), and the cells were not found to expand in the solution (Fig. S2a). Conversely, cell shrinkage was observed due to dehydration and will be discussed later. FBS did not affect the cryoprotection efficiency in either type of freezing medium. Similar trends were found in the mNF and BOSC (Fig. S3). Based on careful evaluation, we conclude that the simple freezing media composed of water and OE₂imC₃C were sufficient to subject to the next experiments.

We investigated the optimum concentration of OE₂imC₃C aqs. By determining the relative numbers of living hNF cells after cryopreservation using water/OE₂imC₃C (95/5–50/50, v/w), we found that water/OE₂imC₃C (90/10 and 85/15, v/w) was the optimal concentration (Fig. 2b). Because OE₂imC₃C is a non-cell-permeable cryoprotectant, dehydration of cells in water/OE₂imC₃C (95/5, v/w) may be insufficient to prevent intracellular ice crystal formation (Fig. S2a). In the cases of water/OE₂imC₃C (65/35, v/w) or higher concentration, the relative number of living cells after cryopreservation decreased as OE₂imC₃C might be toxic at such high concentrations. Rapid afflux and efflux of

water during freezing and recovery are also known to induce damage to cells¹ and they may also be involved. The toxicity of water/OE₂imC₃C (75/25, v/w), despite its very high concentration, is similar to that of the commercial cryoprotectant (Fig. S2c). The osmotic pressure, which is an indicator of cell dehydration, of water/OE₂imC₃C was found to be linearly increased (381, 626, 921, and 1501 mOsm/kg for 95/5, 90/10, 85/15, and 75/25 (w/v), respectively). Cell volume and the reciprocal of the osmotic pressure of the media were reported to display a linear relationship^{1,14}. Herein, the volume of hNF decreased linearly. Similar trends were observed in the cases of mNF and BOSC (Fig. 2c, d) when mNF and BOSC were cryopreserved using water/OE₂imC₃C (95/5–50/50, v/w). Although relative numbers of living cells using OE₂imC₃C aqs. were lower than those using the commercial cryoprotectant, water/OE₂imC₃C (90/10–75/25, v/w) was identified as the optimal concentration range. Therefore, water/OE₂imC₃C (90/10 and 85/15, v/w) was identified as the universal optimal concentration range.

Notably, the relative number of living hNF cells after cryopreservation using water/OE₂imC₃C (95/5, v/w) is significantly different from that observed in the previous study (Fig. S1 vs. the present study Fig. 2b; 1.10 vs 0.46). This is at least partly based on the difference in cell counting methods: an automated cell counter ([®]Countess II FL, Thermo Fisher Scientific) and a hemocytometer in the previous and present studies, respectively. The living cell numbers counted by hemocytometers were lower than those counted by [®]Countess II FL (Fig. S4). [®]Countess II FL is known to show different cell numbers relative to

hemocytometers¹⁵ and is not optimized for counting cells that are partly damaged by cryopreservation. Therefore, we opted to use hemocytometers for subsequent experiments.

Assessment of cell line dependence on cryopreservation with OE₂imC₃C-based freezing media. Here, we cryopreserved hNF, mNF, BOSC, WM, MDA, and PC9 with the optimized water/OE₂imC₃C (90/10, v/w) (Fig. 3a). Even at optimal concentrations, the relative numbers of living cells after cryopreservation were considerably different according to the cell lines. Therefore, we examined the different behaviors of cell lines during cryopreservation.

The toxicity of OE₂imC₃C on the cell lines was investigated (Fig. 3b, c). Single dispersed cells were immersed in water/OE₂imC₃C (90/10, v/w) for 60 min, and the dead cell ratio was measured. Although all cells had higher dead cell ratios in water/OE₂imC₃C (90/10, v/w) than in PBS (Fig. S5a), the maximum dead cell ratio was 35% for WM at room temperature and 16% for mNF at 0 °C; this was insufficient to be directly linked to the low relative number of living cells after cryopreservation (<0.3 for WM). However, the well-cryopreserved cell lines (hNF, MDA, and PC9) showed relatively lower dead cell ratios than poorly cryopreserved cell lines (mNF, BOSC, and WM). Therefore, poorly cryopreserved cell lines might be vulnerable to exposure to OE₂imC₃C. Further discussions are however required before any conclusion can be drawn. For example, poorly cryopreserved cell lines showed high dead cell ratios even in PBS (Fig. S5a). It implies that poorly cryopreserved cell lines were very weak at floating dispersed state.

Non-cell-permeable cryoprotectants, such as OE₂imC₃C, can inhibit extracellular ice crystal formation via direct interaction with water and intracellular ice crystal formation via cell dehydration. According to the literature, it is more important to inhibit intracellular ice crystal formation than extracellular crystals^{1,16}. To investigate dehydration, single dispersed cells were immersed in water/OE₂imC₃C (90/10, v/w), and the cell volumes were measured relative to those in PBS (Fig. 3d, e). All cells shrank in water/OE₂imC₃C (90/10, v/w). In particular, the well-cryopreserved cell lines (hNF, MDA, and PC9) showed significant shrinkage compared with the poorly cryopreserved cell lines (mNF, BOSC, and WM). These different dehydration behaviors were not based on their original cell sizes (Fig. S5b–e). Finally, we found a clear relation between that the water contents of cells in water/OE₂imC₃C (90/10, v/w) and the relative numbers of living cells (Fig. 3f, g and Fig. S5f–i). Therefore, the low cryoprotection efficiency was owing to insufficient cell dehydration, leading to the formation of intracellular ice crystals, as well as toxicity. The insufficient cell dehydration implies that the poorly cryopreserved cell lines contain much amount of low-molecular compounds such as ions. Collectively, these findings highlight the difficulty of achieving sufficient dehydration of all cells using OE₂imC₃C.

Optimization of zwitterion-based freezing media and an in-depth discussion of the cryopreservation mechanism. mNF and BOSC were subjected to cryopreservation using different water/aprotic zwitterion (95/5 and 90/10, v/w) (see Fig. 1 for all structures); this is because other aprotic zwitterions also can strongly interact with water owing to their charges. The cryoprotective effect was found to significantly differ based on the zwitterion species (Fig. 4). The findings indicate that the relative number of living cells after cryopreservation depends on both the zwitterion species and the cell lines. Nevertheless, a clear association between the cryoprotective effect and ionic structures was not found.

Similar non-zwitterionic-type ions, namely free ions called ionic liquids, are known to be toxic^{11,17–19}; however, these ions were subjected to cryopreservation. Surprisingly, the toxic ionic liquid¹³ also exerted a cryopreservation effect at a certain degree (Fig. S7), indicating that toxicity at room temperature might not be related to the cryopreservation efficiency. This finding also implies that toxic compounds can be candidates for cryoprotectants.

The relationship between the osmotic pressures and the molar concentrations of zwitterions in the water/zwitterion (90/10, v/w) was plotted (Fig. S8) to discuss the cryopreservation mechanisms. As a result, a linear relationship was found: the osmotic pressures were related to the concentration but not the ion structure. The relationship between the osmotic pressures and the relative number of living cells (mNF and BOSC) was plotted (Fig. S9); however, no clear relation was found and osmotic pressure was not identified as a dominant factor for cryoprotection.

The physical state, especially glass transition, of water/zwitterion (90/10, v/w) at low temperature was examined using differential scanning calorimetry (DSC); this is because many successful examples based on glass transition have been reported in the case of fast cooling²⁰. Glass transition is related to viscosity¹. In fact, zwitterion solutions have high viscosity due to strong electrostatic interactions and are easy to transform into the glass state^{11,21}. All zwitterion aqs. (90/10, v/w), except for VimC₄S, showed glass transition (Table S1). Glass transition of zwitterion aqs. occurred at –75 to –105 °C. Here, cryopreservation was performed at –85 °C, and therefore, the glass transition temperatures coincidentally existed above and below the temperature. However, no clear relationship was found between the relative number of living cells and the glass transition temperatures (Fig. S10). Furthermore, the relative numbers of living cells were high (mNF and BOSC: 0.63 and 0.45, respectively), even when VimC₄S aq. (90/10, v/w) which did not show glass transition was employed. Such findings suggest that the glass transition itself did not critically affect the cryoprotection effect.

The proportion of unfrozen water of zwitterion aqs. (90/10, v/w) at low temperatures was investigated. Small zwitterions were found to display a higher ratio due to their higher molar concentration. Sulfonate-type zwitterions showed a higher ratio than carboxylate-type zwitterions. An evident tendency was not observed between cell viability and the proportion of unfrozen water (Fig. S11). Therefore, unfrozen water might be necessary for protecting cells from extracellular ice crystals; however, excess amounts of unfrozen water may not exert further cryoprotective effects. Such findings suggest that the species and concentration of zwitterion significantly affect cell viability after cryopreservation; however, glass transition, glass transition temperature, osmotic pressure, and proportion of unfrozen water were not identified as the dominant factors for efficient cryopreservation. Therefore, the critical factors for efficient cryoprotection by zwitterion aqs. are presently under investigation. We also attempted cryopreservation with zwitterion/zwitterion mixtures; however, the blend did not exert synergistic and efficient cryopreservation (Fig. S12).

Optimization via mixing with cell-permeable cryoprotectants. Herein, we reconfirmed the important ability of zwitterions to act as efficient non-cell-permeable cryoprotectants to inhibit extracellular ice formation. The proportion of unfrozen water in the 0.6 mol/L OE₂imC₃C aq. (water/OE₂imC₃C (85/15, v/w)) was 31 wt% at subzero temperature, whereas 11 wt% of the unfrozen water for equimolar sucrose aq., which is a typical non-cell-permeable cryoprotectant. Equimolar DMSO and glycerol aqs.,

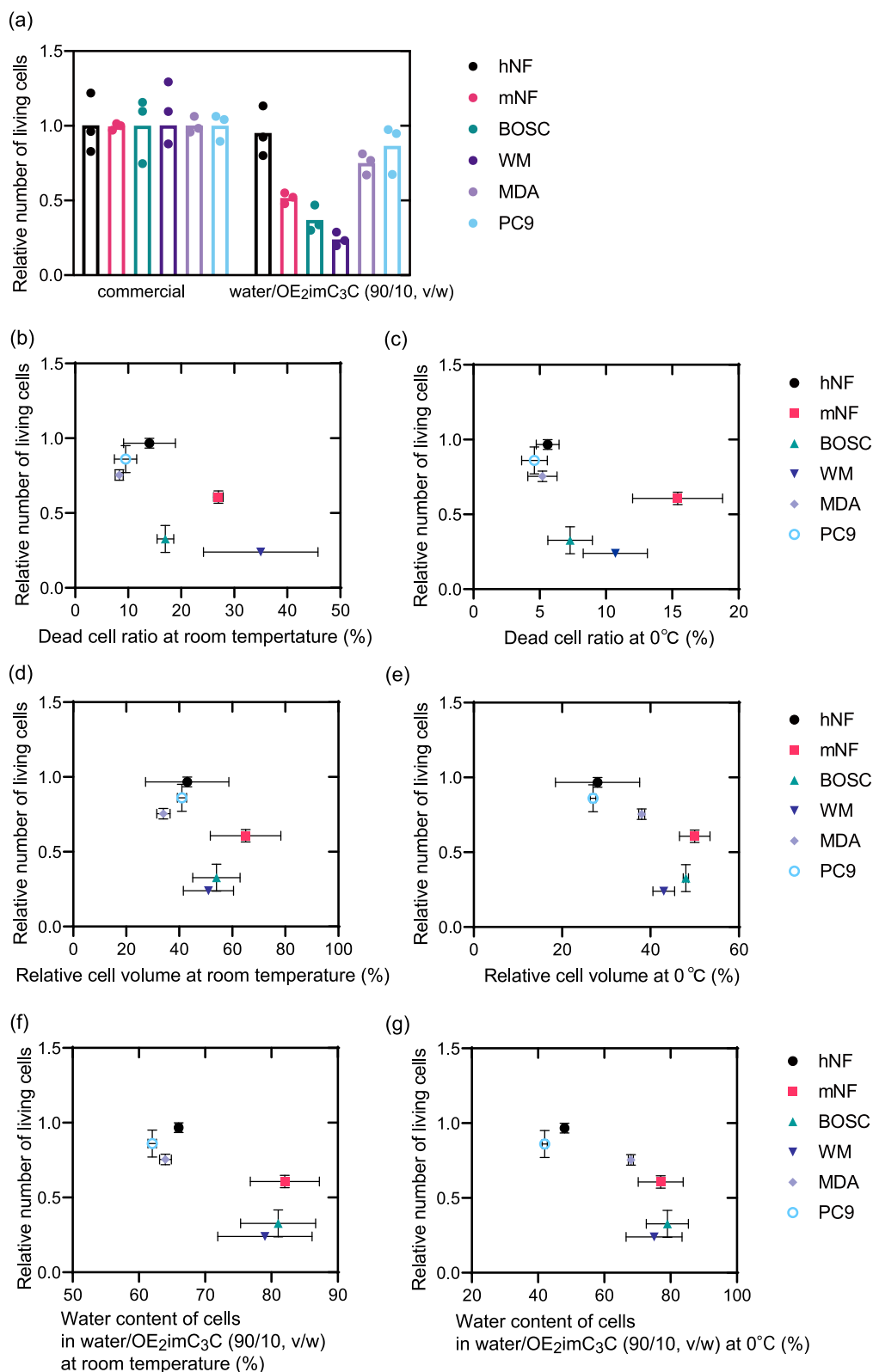


Fig. 3 Cell behaviors in water/OE₂imC₃C (90/10, v/w). **a** Relative number of living cells after cryopreservation with water/OE₂imC₃C (90/10, v/w) ($n = 3$, experimentally triplicate). **b, c** Relation between relative number of living hNF, mNF, BOSC, WM, MDA, and PC9 cells and dead cell ratio at **b** room temperature and **c** 0 °C after 60 min of immersion in the indicated solution ($n = 3$, biologically triplicate). **d, e** Relation between a relative number of living hNF, mNF, BOSC, WM, MDA, and PC9 cells and relative cell volumes at **d** room temperature and **e** 0 °C after 5 min of immersion in the indicated solutions (cell volumes at the same temperature in PBS were standardized as 100%). **f, g** Relation between the water contents of cells in water/OE₂imC₃C (90/10, v/w) at **f** room temperature and **g** 0 °C and the relative numbers of living hNF, mNF, BOSC, WM, MDA, and PC9 cells. ($n = 3$, biologically triplicate). **b-e** These cells were immersed as floating cells in the solutions after trypsinization. The bars show standard error.

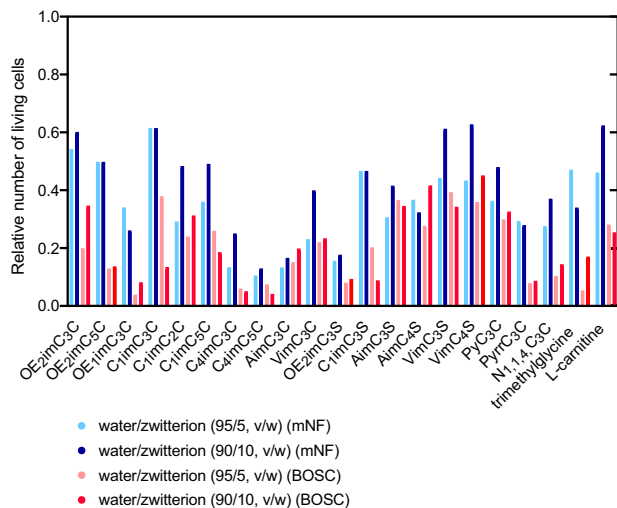


Fig. 4 Relative number of living mNF and BOSC cells after cryopreservation using water/zwitterion (95/5 and 90/10, v/w). ($n = 3$, experimentally triplicate) The actual data points are shown in Fig. S6.

which are typical cell-permeable cryoprotectants with the strong inhibitory ability for extra- and intracellular ice formation, showed 14 and 15 wt% of unfrozen water, respectively. These results clearly suggest that zwitterions are promising non-cell-permeable cryoprotectants.

Blending zwitterions, efficient non-cell-permeating cryoprotectants, and cell-permeating cryoprotectants are expected to exert efficient cryopreservation. DMSO and glycerol were added to water/OE₂imC₃C (90/10, v/w) as additives. As expected, the mixtures resulted in higher relative numbers of living cells (Fig. 5a, b). Water/OE₂imC₃C/DMSO (90/10/15, v/w/w) was identified as the best combination while the relative numbers of living mNF and BOSC cells were 1.13 and 1.14, respectively; these numbers were respectively higher than those of cells cryopreserved with the commercial cryoprotectant. Glycerol is known to be less permeable and highly toxic relative to DMSO¹ aligning with the low relative number of living cells. Adding typical non-cell-permeable cryoprotectants, sucrose, and FBS, into water/OE₂imC₃C (90/10, v/w) did not critically affect the relative number of living cells (Fig. S13), indicating that blending with cell-permeable cryoprotectants is important.

Mixtures of different zwitterions (OE₂imC₃C, VimC₃S, C₁imC₃S, trimethylglycine, L-carnitine) and DMSO were employed. Except for VimC₃S-based freezing media, these mixtures cryopreserved mNF and BOSC in a degree similar to the commercial cryoprotectant. For instance, water/C₁imC₃S/DMSO (90/10/15, v/w/w) led to relative numbers of living mNF and BOSC of 0.92 and 1.01, respectively. Although OE₂imC₃C and VimC₃S without any additives showed similar cryoprotecting effects (see Fig. 4), their cryoprotective effect differed when combined with DMSO; DMSO significantly improved OE₂imC₃C-based media but not VimC₃S-based media. Such findings suggest that the cryoprotective effect of the zwitterion itself is not related to that of mixtures containing DMSO.

Six cell lines presented in Fig. S1 and two cell lines (Vn1919 and HL-60) were cryopreserved using water/zwitterion/DMSO to confirm the universality of the mixtures (Fig. S14). The relative numbers of living cells were found to be improved, including the relative numbers of the cell lines that were poorly cryopreserved by water/zwitterions, such as B16F10 and 4T1. The results suggested that the water/OE₂imC₃C/DMSO (90/10/15, v/w/w) and water/C₁imC₃S/DMSO (90/10/15, v/w/w) were universal cryoprotectants.

The cell lines mentioned above are cryopreserved by the commercial cryoprotectant with high viability, and the high efficiency of water/zwitterion/DMSO is difficult to demonstrate. Here, we cryopreserved two additional cell lines (K562 and OVMANA) that are vulnerable to freezing. Water/zwitterion/DMSO resulted in higher relative numbers of living cells than did the commercial cryoprotectant (Fig. 5e–f). In particular, water/OE₂imC₃C/DMSO and water/C₁imC₃S/DMSO (90/10/15, v/w/w) cryopreserved K562 cells (relative number of living cells: 1.74 and 1.80, respectively). Moreover, both water/zwitterion and water/zwitterion/DMSO cryopreserved OVMANA well. Cell proliferation following cryopreservation with water/OE₂imC₃C/DMSO (90/10/15, v/w/w) and water/C₁imC₃S/DMSO (90/10/15, v/w/w) was found to be equivalent to that with the commercial cryoprotectant (Fig. S15a, b). The water/zwitterion/DMSO mixtures were thus identified as promising freezing media for cell lines or cells that are vulnerable to freezing. As these mixtures consist of only three components, additional inclusions could be made to improve their effects, as commercial cryoprotectants are optimized by blending several additives to adjust pH and osmotic pressure.

Cryoprotecting mechanisms of water/OE₂imC₃C/DMSO. OE₂imC₃C is a non-cell-permeable cryoprotectant that strongly inhibits extracellular ice formation, while DMSO is a cell-permeable cryoprotectant that inhibits intracellular ice formation. To determine the synergistic effect of water/OE₂imC₃C/DMSO, cell volume was measured (Fig. 6a). The water/DMSO mixtures had large cell volumes, suggesting that DMSO requires non-cell-permeable cryoprotectants, such as OE₂imC₃C or NaCl (contained in culture media). Water/OE₂imC₃C/DMSO (90/10/15, v/w/w) exhibited the same cell volume as water/OE₂imC₃C (90/10, v/w). This dehydration inhibited intracellular ice formation. In addition, because DMSO exists in cells, the water content of cells was assumed to be lower in water/OE₂imC₃C/DMSO than in water/OE₂imC₃C. By estimating the toxicity of the freezing media, the water/DMSO mixtures were highly toxic and were associated with cell expansion, as mentioned above. Interestingly, the toxicity of water/OE₂imC₃C/DMSO (90/10/15, v/w/w) was lower than that of medium/DMSO (85/15, v/w) (Fig. 6b). Accordingly, OE₂imC₃C was thought to reduce the toxicity of DMSO. Because water efflux by high osmotic pressure occurs more quickly than DMSO influx, OE₂imC₃C may suppress the influx of DMSO.

Based on previous studies, some cryoprotectants can stabilize cell membranes^{22,23}. Accordingly, a molecular dynamics simulation was conducted to assess the stabilization of the cell membrane (Fig. 6c). In DMSO/water, the cell membrane structure was found to collapse and was partly converted into an interdigitated phase within 250 ns. However, in water/OE₂imC₃C/DMSO, the cell membrane did not critically collapse, even at 1000 ns, despite a certain degree of disruption. The collapse of the lipid membrane was quantitatively assessed by electron density and surface area (Figs. S16 and S17). The electron density of DPPC lipid molecules in the water/DMSO changed from the initial one around the center of the membrane. It indicates that the lipid membrane was transformed into a partly interdigitated structure. On the other hand, the lipid membrane in the water/OE₂imC₃C/DMSO relatively maintained the initial electron density.

The penetration of DMSO molecules can disrupt the organized structure of the lipid bilayer. It was observed that the penetration behavior of DMSO molecules to the lipid bilayer shifted in the presence of OE₂imC₃C (Fig. S18). The number density of DMSO molecules at the center of the membrane was 1.42×10^{-7} and $3.44 \times 10^{-7}/\text{\AA}^3$ in the water/OE₂imC₃C/DMSO and water/DMSO solutions, respectively. The results may be caused by interaction between DMSO and OE₂imC₃C, which is stronger than that

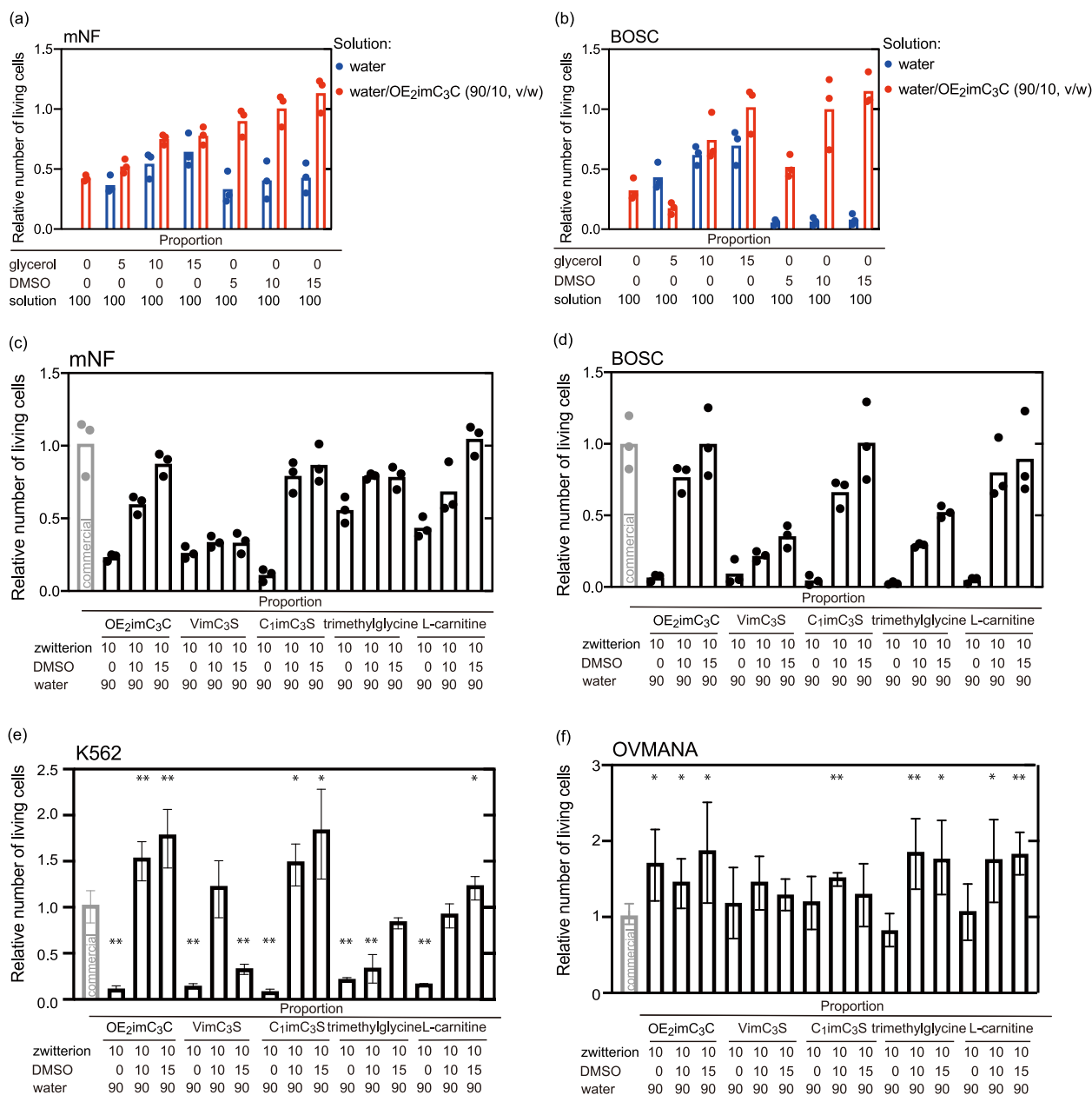


Fig. 5 Cryopreservation of different cells using freezing media containing OE₂imC₃C and cell-permeable cryoprotectants. Relative number of living **a** mNF and **b** BOSC cells after cryopreservation with mixtures of water/OE₂imC₃C (90/10, v/w) and cell-permeable additives (glycerol, DMSO) ($n=3$, experimentally triplicate). A relative number of living **c** mNF, **d** BOSC ($n=3$, experimentally triplicate), **e** K562, and **f** OVMANA ($n=3$, biologically triplicate) cells after cryopreservation with mixtures of water/zwitterion (90/10, v/w) and DMSO. (* $p < 0.1$, ** $p < 0.05$, compared with commercial) The bars show standard error. Total compositions in some cases are over 100 to be clear. The commercial cryoprotectant employed was Culture Sure freezing medium (Fujifilm Wako Pure Chemical Corporation).

between DMSO and DPPC lipid molecules, as shown in Figs. S19 and 20. The interaction between OE₂imC₃C and lipid molecules (Figs. S21–S23) can also contribute to shift in surface charge of cell membrane: we found a slight decrease in the DMSO/lipid interaction and no change in the DMSO/water interaction in the presence of OE₂imC₃C (Fig. S20, 24). From the discussion, OE₂imC₃C interacts with DMSO and lipid and then inhibits the membrane permeation of DMSO, resulting in stabilization of the membrane. This simulation supports one aspect of cryoprotection mechanisms and further study will be required to clarify.

We here suspect that OE₂imC₃C increased the viscosity, which might have affected the simulation results. However, for DMSO

and water molecules, the mean square displacements, which are related to diffusivity, in water/OE₂imC₃C/DMSO was ~80% of that in DMSO/water (Fig. S25). Such findings indicate that viscosity is not a critical factor.

Furthermore, we also analyzed the interaction between OE₂imC₃C/water molecules as shown in Figs. S26. It was observed the water structuring near the anion part of OE₂imC₃C. Hence, it supports the mechanism for cryoprotecting effect: inhibition of ice crystal formation by OE₂imC₃C. Based on these results, OE₂imC₃C may be a promising cryoprotectant that shields cells from the adverse effects of DMSO. The cell lines (K562 and OVMANA) that are vulnerable to freezing could be effectively cryopreserved through the complex mechanisms.

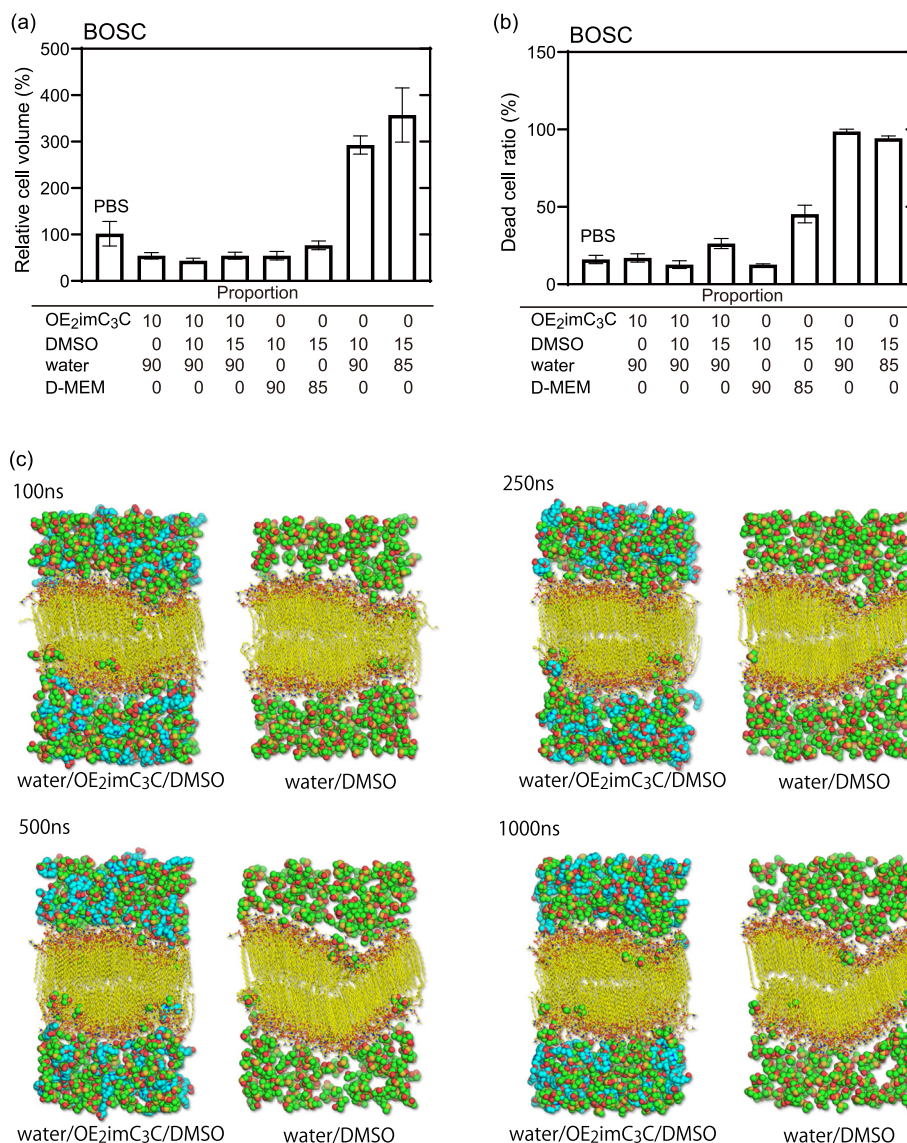


Fig. 6 Cryoprotecting mechanisms of zwitterion/DMSO-containing freezing media. **a** Relative BOSC cell volume after 5 min of immersion in the indicated solutions (cell volume in PBS was standardized as 100%). Total compositions in some cases are over 100 to be clear. **b** Dead BOSC cell ratio after 60 min of immersion in the indicated solution ($n = 3$, biologically triplicate). **a** and **b** The cells were immersed as floating cells in the solutions at room temperature after trypsinization. The bars show standard error. **c** Images of the cell membrane in the water/OE₂imC₃C/DMSO and water/DMSO mixtures at 100, 250, 500, and 1000 ns, as calculated by molecular dynamics simulations with Lipid17 force field. The reproducibility was confirmed by the calculation with Lipid14 force field (Fig. S27).

Conclusion

Herein, zwitterion aqs. were found to exert their cryoprotective effect via cell dehydration, inhibition of extracellular ice formation, and low cytotoxic effects. By altering the structures of the zwitterions, we investigated the impact of the physical properties of the water/zwitterion mixtures. The glass transition, glass transition temperature, osmotic pressure, and proportion of unfrozen water were not identified as the dominant factors for efficient cryopreservation. On the other hand, cell dehydration was found to be a key factor. Although zwitterions were found to be promising non-cell-permeable cryoprotectants, none of the water/zwitterion mixtures resulted in good cryopreservation efficiency for BOSC. As a result, DMSO was blended as a cell-permeable cryoprotectant to compensate for the shortcoming of the non-cell-permeable zwitterions. Water/OE₂imC₃C/DMSO or water/C₁imC₃S/DMSO (90/10/15, v/w/w) was found to cryopreserve different cells. In particular, K562 and OVMANA cells,

which are vulnerable to freezing, were more efficiently cryopreserved with this mixture than with the commercial cryoprotectant. Altogether, OE₂imC₃C was found to strongly inhibit extracellular ice formation and protect cells from the adverse effects of DMSO, resulting in the high cryoprotecting efficiency when mixing with DMSO.

Methods

Materials. OE₂imC₃C, OE₂imC₅C, and C₁imC₃C were synthesized as previously reported¹¹. OE₁imC₃C, C₁imC₅C, C₄imC₃C, C₄imC₅C, AimC₃C, VimC₃C, PyrC₃C, and N_{1,1,4}C₃C were synthesized using a previously reported method with minor modifications¹¹. C₁imC₃S was synthesized as previously reported²⁴. OE₂imC₃S, AimC₃S, AimC₄S, VimC₃S, and VimC₄S were synthesized using a previously reported method with minor modifications²⁴. C₁imC₂C was synthesized as previously reported²⁵. The reagents used to synthesize the above-mentioned zwitterions (2-bromoethyl methyl ether, ethyl 6-bromohexanoate, 1-butylimidazole, 1-allylimidazole, 1-vinylimidazole, 2-bromoethyl methyl ether, 1,3-propene-sultone, pyridine, pyrrolidine, and dimethylbutylamine) were purchased from Tokyo Chemical Industry Co., Ltd., and used as received. Trimethylglycine, 1-

carnitine, and DMSO were purchased from Tokyo Chemical Industry Co., Ltd., and used as received. Glycerol and sucrose were purchased from Nacalai Tesque, Inc., and used as received.

Cell. hNF, mouse normal fibroblast (mNF) derived from C57BL/6-EGFP mice, MDA-MB-231 human breast cancer cells (MDA), WM266.4 human melanoma cells (WM), B16F10 mouse melanoma cells, and 4T1 mouse breast cancer cells were kind gifts from professor Erik Sahai (The Francis-Crick Institute, UK). BOSC human kidney cells, PC9 human lung cancer cells, Mardin-darby canine kidney cells (MDCK) were kind gifts from professor Michiyuki Matsuda (Kyoto University), professor Seiji Yano (Cancer Research Institute of Kanazawa University), and professor Etsuko Kiyokawa (Kanazawa Medical University), respectively. HL-60 human promyelocytic leukemia cells were kindly gifted from professor Atsushi Hirano (Cancer Research Institute of Kanazawa University). K562 human chronic myelogenous leukemia cells and Vn1919 neuroglial and neuronal character co-expressing ependymoma cells were used in the previous studies^{26,27}. OVMANA human ovarian tumor cells were purchased from the Japanese Collection of Research Bioresources.

Cell culture. hNF, mNF, BOSC, WM, MDA, PC9, B16F10, 4T1, and Vn1919 were grown and maintained as monolayer cultures at 37 °C in 5% CO₂ humidified atmosphere, using Dulbecco's modified Eagle's medium (high glucose with L-glutamine and phenol red, Fujifilm Wako Pure Chemical Corporation) supplemented with 1 vol% penicillin–streptomycin solution (×100) (Fujifilm Wako Pure Chemical Corporation) and 10 vol% FBS (Sigma-Aldrich Co., LLC.). HL-60 and K562 were grown and maintained as floating cultures at 37 °C in 5% CO₂ humidified atmosphere, using Roswell Park Memorial Institute medium (RPMI, Nacalai Tesque, Inc.) supplemented with 1 vol% penicillin–streptomycin solution and 10 vol% FBS. OVMANA was grown and maintained as monolayer cultures at 37 °C in 5% CO₂ humidified atmosphere, using RPMI, Nacalai Tesque, Inc. supplemented with 1 vol% penicillin–streptomycin solution and 10 vol% FBS. The cells were sub-cultured every 4–6 days with or without trypsin solution (0.5 w/v% trypsin-5.3 mmol/L EDTA · 4Na solution without phenol red (×10), Fujifilm Wako Pure Chemical Corporation).

Cryopreservation. The zwitterion and zwitterion/DMSO solutions were prepared via mixing with ultrapure water. Thereafter, cells (1 × 10⁶ cells) were collected and centrifuged (100 × g, 5 min at room temperature). After removing the supernatant, 100 μL of cryoprotectants were added and pipetted slowly. The samples were stored in a box (Mr. Frosty, Thermo Fisher Scientific Inc.) in a –85 °C freezer for 3–5 days. For sample thawing, a culture medium incubated at 37 °C was added to the frozen samples. The relative number of living cells was counted using a hemocytometer (Fukaekasei Corporation and Watson Corporation) with trypan blue (Fujifilm Wako Pure Chemical Corporation).

$$\text{Relative number of living cells} = \frac{\text{Counted living cell number (sample)}}{\text{Counted living cell number (commercial cryoprotectant)}}$$

For the proliferation studies, K562 and OVMANA cells after cryopreservation were seeded in a six-well plate. K562 cells were counted sequentially. OVMANA cells were counted after trypsin treatment when the most-grown cells were at 80% confluent.

The commercial cryoprotectant employed was Culture Sure freezing medium (DMSO-containing, Fujifilm Wako Pure Chemical Corporation). This is one of the typical commercial cryoprotectants and is suitable for comparison in cryopreservation efficiency. In the present study, the relative number of living cells was employed because the absolute number of living cells was variable, based on biological variation, even when using the commercial cryoprotectant. The absolute numbers of living cells given by the commercial cryoprotectant were roughly associated with those given by the sample solutions. In addition, most experiments were experimentally triplicated in this study. The results therefore still contain a certain amount of error based on the biological variation but are sufficient to suggest rough trends and relations.

When preparing the freezing medium, the amount of culture medium, FBS, and water were measured by volume using pipettes. The number of zwitterions, DMSO, an ionic liquid, glycerol, and sucrose were measured by weight using an electronic balance unless we note.

Toxicity of cryoprotectants. Cells (1 × 10⁵ cells) after trypsinization were collected and centrifuged (100 × g, 5 min at room temperature). Following the removal of the supernatant, 100 μL of cryoprotectants were added and pipetted slowly. The cells were incubated at room temperature (15–25 °C) and 0 °C as floating cells in cryoprotectants. After 60 min, the dead cell ratio was evaluated by counting using a hemocytometer and trypan blue.

$$\text{Dead cell ratio (\%)} = \frac{\text{Number of dead cells}}{\text{Number of living cells} + \text{Number of dead cells}}$$

Cell volumes in cryoprotectants. Cells (1 × 10⁵ cells) after trypsinization were collected and centrifuged (100 × g, 5 min at room temperature). After removing the

supernatant, 100 μL of cryoprotectants were added and pipetted slowly. Thereafter, the cells were incubated at room temperature (15–25 °C) or 0 °C as floating cells in cryoprotectants. After 5 min, images of the cells were captured with an optical IX83 inverted microscope (Olympus Corporation). The cell radii were measured using the software “ImageJ” (ImageJ 1.52p, Wayne Rasband, National Institutes of Health, USA). Relative cell volumes were calculated using the measured cell radii, relative to the cell volume in phosphate-buffered saline (PBS). Relative cell volume was defined as the following equation.

$$\text{Relative cell volume (\%)} = \frac{\text{Cell volume in water/OE}_2\text{imC}_3\text{C (90/10, v/w) (\mu\text{m}^3)}}{\text{Cell volume in PBS (\mu\text{m}^3)}} \times 100$$

Water content of cells. Cells (1 × 10⁷ cells) after trypsinization were collected and centrifuged (100 × g, 5 min at room temperature). After removing the supernatant, the weight of the cells was measured. Thereafter, the cells were dried in vacuo (1 Pa) and the weight was measured. The water content of original cells and water content of cells in water/OE₂imC₃C (90/10, v/w) was calculated as following equations.

$$\text{Water content of original cells (\%)} = \frac{\text{Cell weight before drying} - \text{Cell weight after drying}}{\text{Cell weight before drying}} \times 100$$

$$\text{Water content of cells in water/OE}_2\text{imC}_3\text{C (90/10, v/w) (\%)} = \frac{\text{Relative cell volume} - (100 - \text{Water content of original cells})}{\text{Relative cell volume}}$$

Osmotic pressure of cryoprotectants. Osmotic pressure was measured using a vapor pressure osmometer (VAPRO 5600; Wescor, Inc., Logan, UT, USA) in the standard 10 mL chamber.

Physical state of cryoprotectants under cryogenic temperature. The phase behavior of the solutions under cryogenic temperature was investigated using DSC (DSC-60A plus, Shimadzu Corporation). DSC measurements were conducted under the following conditions: cooling to –100 °C at a cooling rate of –1 °C/min followed by heating to 25 °C at a heating rate of 5 °C/min. The proportion of unfrozen water in the solutions was estimated from the area of the melting peak at ~0 °C and calculated using the following equation:

$$\text{Proportion of unfrozen water in solution (\%)} = \frac{100 - \frac{\text{Melting heat of the sample solutions [J/g]}}{\text{Melting heat of water (265 J/g)} \times \text{water proportion in the solution}}}{100} \times 100$$

Molecular dynamics simulation. Lipid bilayer contained 200 molecules of 1,2-dipalmitoyl-sn-glycero-3-phosphorylcholine (DPPC) was generated by PACKMOL-Memgen²⁸. The cell membrane was placed at the center in a rectangular periodic box filled with the aqueous solution, where is water slabs with a thickness of 54 Å above and below the lipid bilayer. Simulation systems were constructed with two types of aqueous solution state, water/OE₂imC₃C/DMSO (10,000/94/462 molecules for 75/10/15, w/w/w) and water/DMSO (12,000/480 molecules for 85/15, w/w). Molecular dynamics simulations of the cell membrane systems were carried out using the SANDER and PMEMD.CUDA modules of the Amber18 and AmberTools19 software with the NVIDIA Pascal GPU system²⁹.

The initial positions of water/OE₂imC₃C/DMSO (or water/DMSO) molecules were optimized by 15,000 cycles of steepest descent energy minimization, followed by 10,000 cycles of conjugated gradient minimization, while the structures of the lipid molecules were fixed with the constrained force of 500 kcal/(mol Å²). The whole systems were then subjected to a combination of 15,000 cycles of steepest descent and 10,000 cycles of conjugated gradient energy minimizations. In the subsequent dynamics calculations, the cell membrane system was equilibrated by NVT ensemble simulations with a gradual increase in temperature from –253 to –153 °C at a rate of 0.1 °C/ps, followed by NPT ensemble simulations with a gradual increase in temperature from –153 to 37 °C at a rate of 0.1 °C/ps and pressure of 1 bar. Throughout the heating process, the motion of the lipid molecules was fixed by imposing positional constraints with a constrained force of 10 kcal/(mol Å²). In addition, the NPT ensemble simulations to equilibrate the density of the system were performed for a total of 5 ns by repeating ten times at constant temperature (37 °C) and pressure (1 bar). Finally, the production simulations were carried out for 1 μs at constant temperature (37 °C) and pressure (1 bar).

The TIP3P model was used for the water molecules, and the lipid molecules were described by the Lipid17 force field³⁰. DMSO and OE₂imC₃C molecules were modeled using the general AMBER force field³¹. The temperature and pressure of the system were regulated by a Langevin thermostat with a collision frequency of 1 ps^{–1} and a Berendsen barostat, respectively. The molecular dynamics simulation was performed using a 2 fs integration time step coupled with the SHAKE option. The particle mesh Ewald method was adopted for long-range interactions, and the cutoff for non-bonding interactions in the coordinate space was fixed at 10 Å.

Reporting summary. Further information on research design is available in the Nature Research Reporting Summary linked to this article.

Data availability

All data are available in the main text or supplementary materials.

Received: 25 May 2021; Accepted: 6 October 2021;

Published online: 28 October 2021

References

- Wolkers, W. F. & Oldenhof, H. *Cryopreservation and freeze-drying protocols*. (Springer, 2015).
- ATCC. <https://www.Atcc.Org/products>.
- Pegg, D. E., Wang, L. & Vaughan, D. Cryopreservation of articular cartilage. Part 3: the liquidus-tracking method. *Cryobiol* **52**, 360–368 (2006).
- Chang, T. & Zhao, G. Ice inhibition for cryopreservation: materials, strategies, and challenges. *Adv. Sci.* **8**, 2002425 (2021).
- Qin, Q. et al. Addition to “bioinspired L-proline oligomers for the cryopreservation of oocytes via controlling ice growth”. *ACS Appl. Mater. Interfaces* **12**, 56661–56661 (2020).
- Cheng, Y., Yu, Y., Zhang, Y., Zhao, G. & Zhao, Y. Cold-responsive nanocapsules enable the sole-cryoprotectant-trehalose cryopreservation of beta cell-laden hydrogels for diabetes treatment. *Small* **15**, e1904290 (2019).
- Chang, T. et al. Synergistic ice inhibition effect enhances rapid freezing cryopreservation with low concentration of cryoprotectants. *Adv. Sci.* **8**, 2003387 (2021).
- Zhang, Y. et al. Cold-responsive nanoparticle enables intracellular delivery and rapid release of trehalose for organic-solvent-free cryopreservation. *Nano Lett.* **19**, 9051–9061 (2019).
- Suzuki, T., Komada, H., Takai, R., Arii, K. & Kozima, T. T. Relation between toxicity of cryoprotectant dmso and its concentration in several fish embryos. *Fish. Sci.* **61**, 193–197 (1995).
- Oh, K. I., Rajesh, K., Stanton, J. F. & Baiz, C. R. Quantifying hydrogen-bond populations in dimethyl sulfoxide/water mixtures. *Angew. Chem. Int. Ed.* **129**, 11533–11537 (2017).
- Kuroda, K. et al. Design of wall-destructive but membrane-compatible solvents. *J. Am. Chem. Soc.* **139**, 16052–16055 (2017).
- Satria, H., Kuroda, K., Tsuge, Y., Ninomiya, K. & Takahashi, K. Dimethyl sulfoxide enhances both the cellulose dissolution ability and biocompatibility of a carboxylate-type liquid zwitterion. *N. J. Chem.* **42**, 13225–13228 (2018).
- Kuroda, K. et al. Non-aqueous, zwitterionic solvent as an alternative for dimethyl sulfoxide in the life sciences. *Commun. Chem.* **3**, 1–7 (2020).
- Pegg, D., Hunt, C. & Fong, L. Osmotic properties of the rabbit corneal endothelium and their relevance to cryopreservation. *Cell biophys.* **10**, 169–189 (1987).
- Countess II FL, Thermo Fisher Scientific <https://www.thermofisher.com/jp/ja/home/brands/product-brand/countess-automated-cell-counter.html> (2020).
- Lovelock, J. Het mechanism of the protective action of glycerol against haemolysis by freezing and thawing. *Biochim. Biophys. Acta* **11**, 28–36 (1953).
- Lee, S. M., Chang, W. J., Choi, A. R. & Koo, Y. M. Influence of ionic liquids on the growth of *Escherichia coli*. *Korean J. Chem. Eng.* **22**, 687–690 (2005).
- Zhao, D., Liao, Y. & Zhang, Z. Toxicity of ionic liquids. *CLEAN – Soil, Air, Water* **35**, 42–48 (2007).
- Lim, G. S., Zidar, J., Cheong, D. W., Jaenicke, S. & Klähn, M. Impact of ionic liquids in aqueous solution on bacterial plasma membranes studied with molecular dynamics simulations. *J. Phys. Chem. B* **118**, 10444–10459 (2014).
- Rajan, R., Hayashi, F., Nagashima, T. & Matsumura, K. Toward a molecular understanding of the mechanism of cryopreservation by polyampholytes: Cell membrane interactions and hydrophobicity. *Biomacromolecules* **17**, 1882–1893 (2016).
- Yoshizawa-Fujita, M., Tamura, T., Takeoka, Y. & Rikukawa, M. Low-melting zwitterion: Effect of oxyethylene units on thermal properties and conductivity. *Chem. Commun.* **47**, 2345–2347 (2011).
- Leslie, S. B., Israeli, E., Lighthart, B., Crowe, J. H. & Crowe, L. M. Trehalose and sucrose protect both membranes and proteins in intact bacteria during drying. *Appl. Environ. Microbiol.* **61**, 3592–3597 (1995).
- Bailey, T. L. et al. Synthetically scalable poly(ampholyte) which dramatically enhances cellular cryopreservation. *Biomacromolecules* **20**, 3104–3114 (2019).
- Ito, Y., Kohno, Y., Nakamura, N. & Ohno, H. Addition of suitably-designed zwitterions improves the saturated water content of hydrophobic ionic liquids. *Chem. Commun.* **48**, 11220–11222 (2012).
- Blackburn, G. M. & Dodds, H. L. Strain effects in acyl transfer reactions. Part iii. Hydroxide and buffer-catalysed hydrolysis of small and medium ring lactones. *J. Chem. Soc., Perkin Trans. 2*, 377–382 (1974).
- Dewi, F. R. P. et al. Nucleoporin TPR (translocated promoter region, nuclear basket protein) upregulation alters mtor-hsf1 trails and suppresses autophagy induction in ependymoma. *Autophagy* **17**, 1001–1012 (2020).
- Funasaka, T. et al. Rna export factor rae1 contributes to nup98-hoxa9-mediated leukemogenesis. *Cell Cycle* **10**, 1456–1467 (2011).
- Schott-Verdugo, S. & Gohlke, H. Packmol-memgen: A simple-to-use, generalized workflow for membrane-protein-lipid-bilayer system building. *J. Chem. Inf. Model* **59**, 2522–2528 (2019).
- Amber 18. (University of California, San Francisco, 2018).
- Dickson, C. J. et al. Lipid14: the amber lipid force field. *J. Chem. Theory Comput.* **10**, 865–879 (2014).
- Wang, J., Wolf, R. M., Caldwell, J. W., Kollman, P. A. & Case, D. A. Development and testing of a general amber force field. *J. Comput. Chem.* **25**, 1157–1174 (2004).

Acknowledgements

We thank Ms. S. Yamagishi (Hirata Laboratory) for her technical assistance. This study was partly supported by ACT-X (for K.K., JPMJAX1915 from Japan Science and Technology Agency), A-STEP (from Japan Science and Technology Agency), KAKENHI (18K14281 for K.K. and 17K07181 for E.H. from the Japan Society for the Promotion of Science), the Leading Initiative for Excellent Young Researchers (for K.K., from the Ministry of Education, Culture, Sports, Science and Technology-Japan), and Kanazawa University SAKIGAKE project 2020.

Author contributions

Yui Kato: methodology, validation, investigation, writing—original draft. Takuya Uto: Investigation, Writing—review & editing. Daisuke Tanaka: investigation. Kojiro Ishibashi: investigation, methodology. Akiko Kobayashi: resources, methodology, investigation. Masaharu Hazawa: methodology, investigation. Richard W. Wong: resources, methodology, investigation. Kazuaki Ninomiya: discussion, writing—review & editing. Kenji Takahashi: discussion, writing—review & editing. Eishu Hirata: resources, conceptualization, project administration, supervision, writing—review & editing, funding acquisition. Kosuke Kuroda: resources, conceptualization, project administration, supervision, writing—original draft & review & editing, funding acquisition.

Competing interests

The authors declare no competing interests.

Additional information

Supplementary information The online version contains supplementary material available at <https://doi.org/10.1038/s42004-021-00588-x>.

Correspondence and requests for materials should be addressed to Eishu Hirata or Kosuke Kuroda.

Peer review information *Communications Chemistry* thanks Ananya Debnath, Gang Zhao, and the other, anonymous, reviewer(s) for their contribution to the peer review of this work.

Reprints and permission information is available at <http://www.nature.com/reprints>

Publisher's note Springer Nature remains neutral with regard to jurisdictional claims in published maps and institutional affiliations.



Open Access This article is licensed under a Creative Commons Attribution 4.0 International License, which permits use, sharing, adaptation, distribution and reproduction in any medium or format, as long as you give appropriate credit to the original author(s) and the source, provide a link to the Creative Commons license, and indicate if changes were made. The images or other third party material in this article are included in the article's Creative Commons license, unless indicated otherwise in a credit line to the material. If material is not included in the article's Creative Commons license and your intended use is not permitted by statutory regulation or exceeds the permitted use, you will need to obtain permission directly from the copyright holder. To view a copy of this license, visit <http://creativecommons.org/licenses/by/4.0/>.

© The Author(s) 2021